sustainability

MDPI

Article

GRIDMAT—A Sustainable Material Combining Mat and Geogrid Concept for Ballasted Railways

M. Sol-Sánchez *, T. Mattinzioli, J. M. Castillo-Mingorance, F. Moreno-Navarro and M. C. Rubio-Gámez

Laboratory of Construction Engineering, University of Granada, C/Severo Ochoa s/n, 18071 Granada, Spain
* Correspondence: msol@ugr.es

Abstract: Under ballast mats (UBM) have demonstrated their capacity to reduce section stiffness and ballast degradation. However, UBM can cause ballast destabilisation under some circumstances due to excessive vertical track deflections, requiring the installation of geogrids over the mat which increases costs and time. As alternative to this solution, this paper shows the design of GridMat: a sustainable technology for ballasted railways that combines the concepts of geogrids and under ballast mats (UBM) manufactured from recycled crumb rubber. This aims to provide damping capacity while limiting the oscillations and settlement of ballast layer. To obtain the optimal GridMat design, five different configurations varying the aperture size and void areas were assessed through laboratory box tests reproducing the track section including the GridMat. Results showed that the optimal Gridmat was of 55 mm aperture seize and 25% void area. To evaluate the sustainability of this design, the expected number of conservation and renewal operations were calculated from full-scale laboratory tests and a life-cycle assessment and life-cycle cost analysis were undertaken. GridMat showed long-term reduction in ballast degradation and track settlement, reducing need for maintenance and renewal operations in comparison with standard mats.

Keywords: geogrid; mat; railway; laboratory testing; box test; LCA

Citation: Sol-Sánchez, M.; Mattinzioli, T.; Castillo-Mingorance, J.M.; Moreno-Navarro, F.; Rubio-Gámez, M.C. GRIDMAT—A Sustainable Material Combining Mat and Geogrid Concept for Ballasted Railways. *Sustainability* **2022**, *14*, 11186. https://doi.org/10.3390/su141811186

Academic Editor: Marco Guerrieri

Received: 25 July 2022
Accepted: 29 August 2022
Published: 7 September 2022

1. Introduction

Under ballast mats (UBM) offer the ability to adapt railway structure flexibility and damping capacity according to certain track requirements. UBM are designed to filter vibrations in urban areas and to reduce section stiffness and fast ballast degradation in structures such as bridges, tunnels, underpasses; these structures are often subjected to accelerated ballast abrasion and breakage due to high stress levels on the sub-base due to excessive track stiffness. Based on the specific functional requirements of the UBM, these components must be designed and composed of materials able to provide optimum static and dynamic track performance. Thus, their characteristic design property is their dynamic elasticity, commonly expressed as the bending modulus ranging mainly between 0.03 N/mm^3 and 0.22 N/mm^3 (with a reference axle load of 22.5 t in standard tracks with concrete sleepers spaced 60 cm apart over a ballast layer in concrete tunnels) [1,2].

Numerous studies have been carried out during the last few years using UBM, finding efficient solutions from rubber-based mats for vibration isolation while reducing deformation and abrasion in both ballasted and ballastless systems. For example, previous authors [3] demonstrated the effectiveness of mats for gradually changing the vertical stiffness in transition zones between different slab tracks. Other studies [4] focused on the capacity of the mats to improve the service performance of track sections including various isolation layers. Additionally, it has been shown that UBM can be viably manufactured from recycled rubber [5,6], which would reduce raw material and energy consumption. The long-term structural properties of using recycled rubber have also been demonstrated [7,8]. Nonetheless, despite these advantages of UBM, some negative aspects must be also considered, such as the economic costs and environmental impacts associated with the mat and its installation.

Another disadvantage of UBM is associated with the possible ballast destabilisation that can take place due to excessive vertical track deflections if mats are installed over supports not rigid enough. This was mainly found when using mats with relatively low bending moduli and/or over platforms with relatively low bearing capacity. In fact, authors such as Raymond and Bathurst [9] showed that the ballast settlement increases with decreasing bottom stiffness, being confirmed by other researchers [6,10,11] that showed how the application of UBM could accelerate ballast settlement and the rate of ballast layer deformation in the short- and long-term. This could be associated with the higher oscillation of ballast particles, in turn impeding layer compaction particularly over weak platforms. Therefore, this increased the demand for maintenance operations, which has the opposite intended effect for UBM.

In response to possible ballast destabilisation from UBM, the use of a geogrid in combination with mats has been seen as a possible solution. The use of geogrids has started to gain popularity as a low-cost solution for lateral ballast stabilization. Hussaini et al. [12] found that geogrids reduced the lateral spreading of ballast, the extent of permanent vertical settlement, and minimised ballast particle breakage, at vertical stresses of both 230 and 460 kPa. Esmaeili et al. [13] found from both lab and field tests that the use of one or two geogrid layers would increase the lateral resistance of ballast layers. These benefits of geogrids could result in a reduction in maintenance operation requirements, and in turn economic costs. Brown et al. [14] found that from both laboratory and in-field tests that geogrids could offer a three-fold reduction in tamping operation requirements. In contrast to such benefits, some disadvantages must be also considered for the use of geogrids over mats when aiming to reduce problems associated with ballast destabilization. In this sense, some authors [14,15] found that geogrid are effective only when using appropriate design factors, mainly related to aperture size. In fact, it has been demonstrated that an ideal aperture size must account for adequate ballast particle interlocking [16], which demand for specific studies into this issue. In addition, it is important to note that the addition of geogrids over mats, joined to provide flexibility while confining ballast particles, would increase installation costs and environmental impacts, which is opposite to social demand.

In this context, this research focuses on the development of a new material for ballasted tracks combining the concept of mats and geogrids by designing elastic layers as mats directly including apertures. This material aims to reproduce, in a sole track component, the functions of mats (flexibility, damping capacity, etc.) while allowing for confining ballast aggregates to avoid the phenomena of ballast destabilisation. Furthermore, they are manufactured from recycled rubber to enhance the sustainable aspect. This material aims to reproduce the functions of mats (flexibility, damping capacity, etc.) while allowing for confining ballast aggregates to avoid the phenomena of ballast destabilisation.

This material was named GridMat (GM), given its aim to combine the benefits of grids and mats, while reducing the negative aspects associated with ballast destabilisation over mats. For this purpose, this paper presents the design study into this solution by evaluating the impact of key parameters such as the aperture size of the aperture, total aperture area on section performance, while also carrying out life-cycle assessments (LCA) and life-cycle cost analyses (LCCA) for the proposed solutions manufactured from recycled rubber to reduce environmental impacts. Results were compared with standard track sections (both with and without standard UBM), while also understanding the impacts of the GM design, including those associated with maintenance and renewal requirements for each solution.

2. Methodology

This methodology section describes the materials used in the laboratory tests to analyse the effect of GridMat on track section performance, while presenting the testing plan and methods applied during the laboratory step and the LCA and LCCA assessment.

2.1. Materials

Two elastic mats made from recycled crumb rubber from end-of-life tyres were used for studying the GridMat solution (Figure 1). Mats with thicknesses of 7 mm and 11 mm were implemented, to provide a dynamic stiffness at 10 Hz ($C_{dyn10Hz}$) close to 0.10 N/m^3 and 0.07 N/mm^3, respectively, according to DIN 45673-5 [17] when tested under a ballasted plate, and 0.45 N/mm^3 and 0.30 N/mm^3 when tested between two flat metallic plates according to DBS 918 071-1 [18].

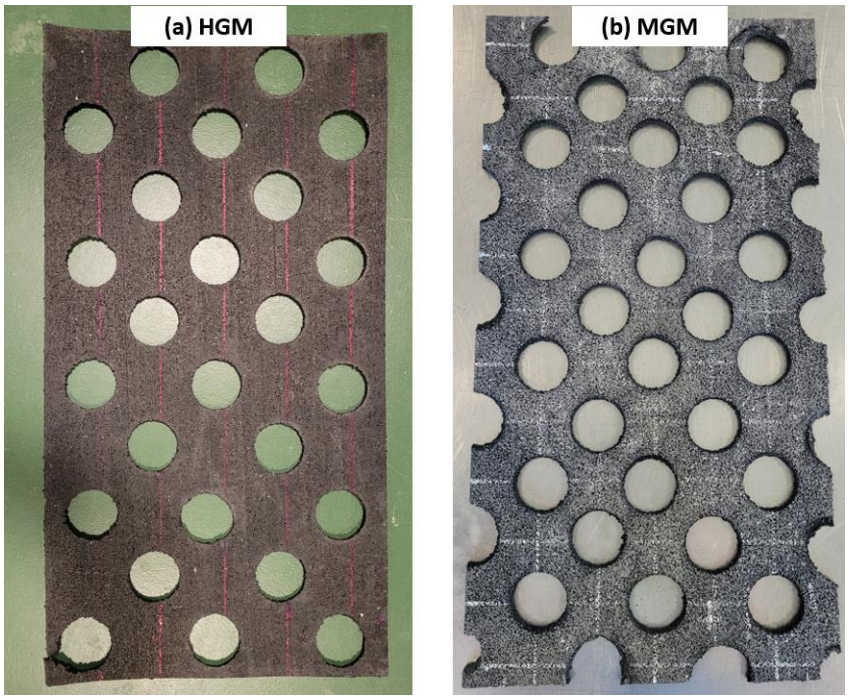

Figure 1. Example of the (**a**) hard—HGM; and (**b**) medium—MGM GridMats studied, with diameter of 50 mm.

These mats could be considered as medium (MM) and hard (HM) mats, selected for being considered the most favourable conditions against ballast destabilisation caused by excessive vertical track deflections when using soft and very soft mats [1]. From these standard mats (HM and MM), different GridMat designs were studied with varying circular aperture combinations, being named as HGM and MGM corresponding to Hard and Medium GridMat with 7 mm and 11 mm of thickness, respectively.

Additionally, for testing the impact of mats and their design on track section performance, a ballast box was used in this study at laboratory level. This was selected since this type of test over a full-scale section reproduced in controlled conditions have demonstrated to be appropriate to compare solutions and/or calibrate models [19]. This testing box was 440 mm wide, 750 mm long, and 500 mm heigh, permitting the complete study of the under-rail seat area where higher stress and deflections are expected. To reproduce the track section, a concrete sleeper section (250 mm width at the bottom, and 320 mm of length) and a rail section, type UIC-54 (250 mm long), fastened by a VM-type system (equipped with clips and a pad with 7 mm of thickness and 125 kN/mm of static stiffness [20]) were placed over a 30 cm thick ballast layer. The ballast used was composed of ophite aggregates from 31.5 mm to 63 mm, fitting the physical and mechanical requirements for this material according to the EN 13450 [21].

2.2. Testing Plan and Methods

The testing plan carried out is shown in Table 1, aiming to define the influence of gridmat design on its capacity to reduce track settlement while providing an elastic solution.

In particular, the plan was divided into 2 main study steps: (1) GridMat design through laboratory tests where it was analysed (1.1) the effect of aperture size of the apertures and (1.2) the influence of the number of apertures or distance between them (in fact, the effect of aperture area per m^2 of mat); (2) GridMat viability across its life-cycle through the (2.1) calculation from previous results in step 1 and 2 of predictable maintenance and renewal operations for a track over 50 years, and (2.2) LCA and LCCA for the GridMat in comparison to standard track solutions.

Table 1. GridMat testing plan.

Study Step	Tested Property	Tested Material	Test
GridMat design	Aperture size (Diameter values in mm) 25, 40, 50, 60, 70	No mat—NM Hard mat—HM Medium mat—MM Hard GridMat—HGM Medium GridMat—MGM	Ballast box test in laboratory measuring: - relative settlement (%), - vertical stiffness modulus (N/mm^3) - and settlement ratio per load cycle (SRLC, mm/cycle)
	Number of voids per m^2 80, 100, 160 *(Void area per m^2 in %, 15, 25, 35)*	NM HM HGM	
GridMat viability across its life-cycle	Comparing requirements of maintenance/renewal operations	NM HM HGM	Simulation of number of operations required in a period for each case
	Environmental and economic life-cycle assessment		LCA and LCCA

2.2.1. GridMat Design

The first study step consisted of assessing the influence of the size of the apertures on the mechanical performance when using the grid mat (Figure 2), in comparison to the reference solution (without mat—NM) and to the cases with standard mats (hard and medium mat without apertures, HM and MM, respectively). For this purpose, the diameter of the apertures in the grid mat was varied between 25 mm, 40 mm, 50 mm, 60 mm, and 70 mm. These sizes were considered in reference to previous studies [14], focused on assessing the design of geogrids for railways, and finding apertures around 35–65 mm in diameter could be considered appropriate. Therefore, in this study such value was assessed while also studying a wider range to analyse the effect when applied in an elastic mat. This analysis was carried out for the hard and medium GridMats (7 mm and 11 mm thick, respectively) in order to study the influence of the grid size on two different elastic solutions.

The second study step focused on assessing the influence of the area of apertures per m^2 on section performance (Figure 2), which was obtained by varying the distance between apertures, and therefore, considering a different percentage of voids in the mat which could modify the damping capacity of the mat. For this, the step focused on the hard GridMat with an aperture size of 50 mm (selected from previous results in stage 1, as an example of GridMat to analyse the impact of aperture number). The variable of number of apertures per m^2 ranged from 80, 100, and 160, corresponding to void areas of 15%, 25%, and 35%. These solutions were compared with the standard hard mat (used as an elastic reference, with 0 apertures and 0% of void area) and with the conventional track without mat (with no mat, and therefore, 100% of void area).

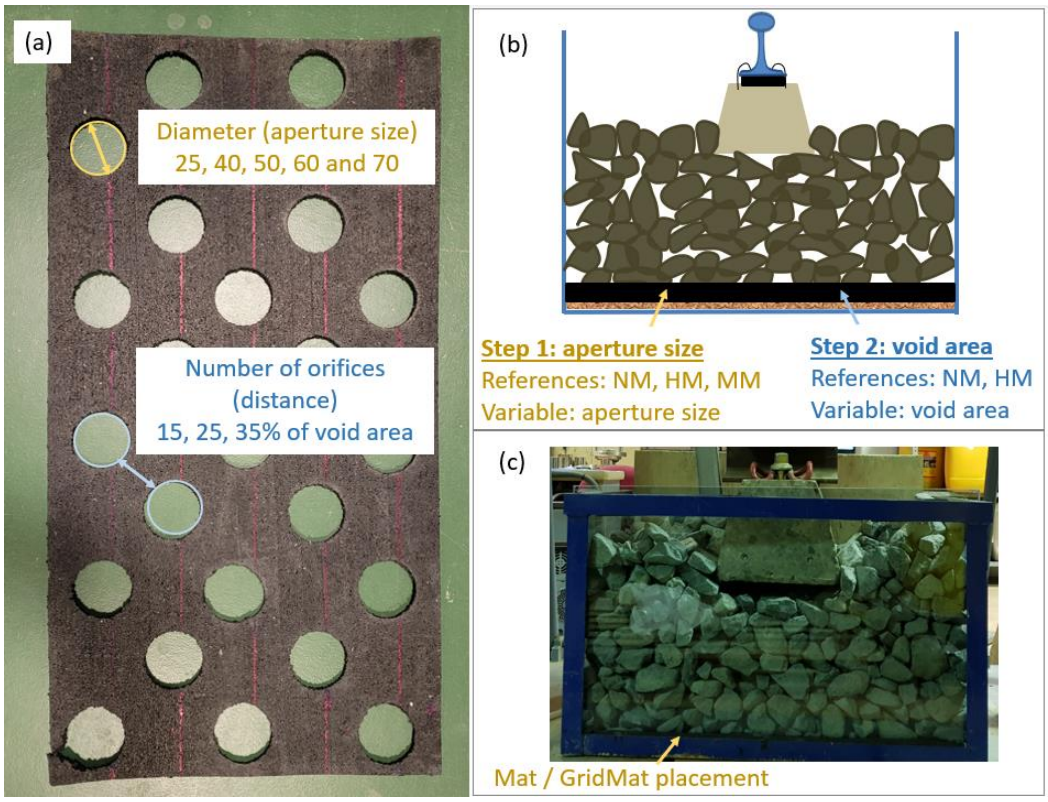

Figure 2. Description of laboratory test: (**a**) image of an example of GridMat indicating the tested parameters; (**b**) scheme of laboratory test configuration describing the laboratory steps; (**c**) image of laboratory test and mat/GridMat position.

To study these first two stages on GridMat design, a series of ballast box tests were carried out in a laboratory by reproducing a number of track sections including the different elastic solutions under the ballast layer. For the cases using the elastic solutions (standard mats or GridMats), these elements were placed under the ballast layer (showed in Figure 2c) which had a thickness of 30 cm from the bottom of the sleeper. Therefore, this paper aims to compare GridMat with standard mats by placing both under the ballast layer. In addition, this placement for the GridMat during this study was selected aiming to avoid possible modifications in the construction process that could take place during installation of the GridMat if it would be used in the middle of the ballast layer, as well as the possible further incidences during maintenance operations (such as tamping) during the service life.

The configuration of the test is as described in previous studies [22,23], consisting of applying 200,000 loading cycles at 5 Hz over the rail head (vertical loads) under a stress range close to 250 kPa under the sleeper, which can be considered appropriate for reproducing field conditions according to previous studies [24,25] when using the load between bogies as predominant. In addition, these testing parameters and box configurations have been proven to reproduce section conditions appropriate for the comparative study aimed in this research, while presenting comparable effect to that obtained in other studies [10,11] using more complex facilities and tools to analyse the impact of mats and other configurations reproducing real field performance.

The parameters assessed for each testing configuration were: (1) the relative settlement measured between the final ballast deformation and such obtained after the ballast compaction during the first 1000 loading cycles; (2) vertical stiffness modulus (N/mm^3) calculated as the section stiffness (kN/mm) per sleeper section area (mm^2), aiming to obtain comparable results regardless of the testing box size; (3) and the settlement ratio per load cycle (SRLC, in mm/cycle) as the trend to settlement measured during the final

50,000 loading cycles when the section performance was considered stable, in agreement with previous studies also analysing SRLC [22,23].

2.2.2. GridMat Viability across Its Life-Cycle

The impact of GridMat during its service life was analysed by calculating the effect of using this material on the frequency of requirements for track maintenance and renewal operations, while later calculating the environmental and cost life-cycle assessment.

Maintenance Requirements

The third study stage consisted of estimating track maintenance (tamping) and rehabilitation (superstructure) operations during a 50-year service life with a traffic level of 20 MGT (million gross tonnes transported), used as an example from real traffic conditions according to previous studies [26]. Based on the results from the testing in steps 1 and 2, this analysis was carried for the reference conventional solution (conventional track without mat, NM), the hard mat (reference mat without apertures, HM), and for the high-stiffness GridMat (with a thickness of 7 mm, HGM) with multiple aperture and void area arrangements.

For this analysis, it was calculated through the expected track geometry degradation, via the Standard Deviation (SD) calculated from the box test results by using a linear empirical law (Equation (1)). This method and equation have been stated in previous literature [24] as appropriate for the estimation of geometrical track degradation under traffic effect. In addition, this index was used in this study since rail authorities commonly plan maintenance interventions based on SD index, following the limits established in EN 13848-5 [27] (showed in Table 2). This is used because of its ability to define track quality and the level of differential ballast settlement, which is essential in safety and comfort. To determine this index from laboratory results, Equation (1) presents a linear empirical law since an extensive literature review [28,29] revealed that this is the best correlation with field data:

$$SD\ (\text{mm}) = A + C \times T \quad (1)$$

where:

- SD is the Standard Deviation (in mm) of longitudinal level as indicated in EN 13848-5 [25];
- A is the initial value of standard deviation (associated with maintenance efficiency);
- C is the coefficient of cumulative settlement ratio under traffic loads, measured as mm/MGT;
- T is the level of traffic, considered as 20 MGT in this study.

Table 2. Permissible standard deviation (SD) levels, according to the EN 13848-5 [27].

Train Speed Limit (km/h)	Longitudinal Level AL, Standard Deviation (SD)—EN 13848-5	
	Minimum Limit (mm)	Maximum Limit (mm)
≤80	2.3	3.0
≤120	1.8	2.7
≤160	1.4	2.4
≤230	1.2	1.9
≤300	1.0	1.5

In this study, parameter A was fixed at a value of 5% from the limits of SD (established from EN 13848-5, depending on speed as seen in Table 2), which is in consonance with previous studies and experiences assuming a value of 95% as effectiveness of maintenance [29]. Parameter C was calculated from the SRLC (mm/cycle) results obtained in the ballast box tests, being converted to SD values by using a correlation factor between settlement and a

SD of 0.06 as defined by the British railway lines [30]. Therefore, the *C* value was calculated as follows (Equation (2)):

$$C_i[\text{mm/MGT}] = SRLC_i\left[\frac{\text{mm}}{\text{cycle}}\right] \times \frac{1,000,000[\text{cycles}]}{25[\text{tons}]} \times 0.06 \quad (2)$$

being:

- C_i the case analysed (reference, HM, or HGM with different aperture sizes and void areas);
- $SRLC_i$ the settlement ratio (mm/cycle) obtained in the box tests for each study case;
- 1,000,000 is the number of cycles considered for a million loads;
- 25 is the axle load (in tons) considered during the box test.

The factor considered to convert settlement results into *SD* values is 0.06, according to previous experiences [30]. This methodology has also been used in previous research [26] for comparative studies between different solutions.

Once calculated, the *SD* value per year for each solution (under an annual traffic of 20 MGT) was compared with the minimum and maximum *SD* limit fixed in EN 13848-5 (Table 2), for speeds between 80 km/h and 300 km/h. From this, the number of years between each maintenance operation (tamping and ballast stabilizer) as well as maintenance frequency (calculated as 1/years between required operations) were estimated, in order to analyse the impact of each solution.

The renewal frequency was calculated for an analysis period of 50 years, establishing the degradation limit thus requiring renewal operation from considering the increase in the quantity of ballast particles with a size lower than 22.4 mm due to traffic actions and maintenance operations. In previous studies carried out by the authors of this paper [10], using the same railway facilities and materials, it was seen that the factor of ballast degradation under traffic was equal to 1.44 (%/MGT) for a conventional track and 0.89 (%/MGT) when using elastic mat under the ballast. In addition, in other previous studies from the authors [31], a ballast degradation factor (calculated as a percentage of increase in particles lower than 22.4 mm) of 1.18 (%/operation) was found for each tamping operation simulation under the rail seat area. Therefore, considering such factors, the ratio of ballast degradation was calculated as follows (Equation (3)):

$$D_i(\%) = TD_i \times T + MD_i \times N_i \quad (3)$$

where:

D_i is the level of degradation for each case study of this research, expressed as percentages of particles lower than 22.4 mm;

TD_i is the ballast degradation factor due to traffic for each solution, with or without a mat (in %/MGT);

T is the level of traffic, considered in this study as 20 MGT;

MD_i is the ratio of ballast degradation due to tamping operation (established in 1.18%/operation);

N_i is the number of operations required in 50 years, determined in the previous step from box test results and SD limits. Note that for this comparative study a linear ballast degradation and constant period between maintenance operations during the aperture traffic life was considered. This was considered as appropriate for a comparative study.

From the results of the ballast degradation for each solution, calculated as an accumulation of percentage of particles lower than 22.4 mm, the number of renewal operations required during a period of 50 years was calculated. This was achieved by comparing value D_i with a maximum limit of 30%, which is a reference in previous studies [32].

Environmental and Economic Life-Cycle Assessment

In the fourth testing stage, six LCA and LCCA simulations were carried out to determine the viability of the GridMat over a 50-year analysis period. The life-cycle analyses

were undertaken with a full life-cycle perspective, considering resource extraction, composite material production, construction, maintenance, and rehabilitation (stages A1–A5, B2 and B4, according to EN 15804 [33]). The system boundaries of the current study are shown in Figure 3.

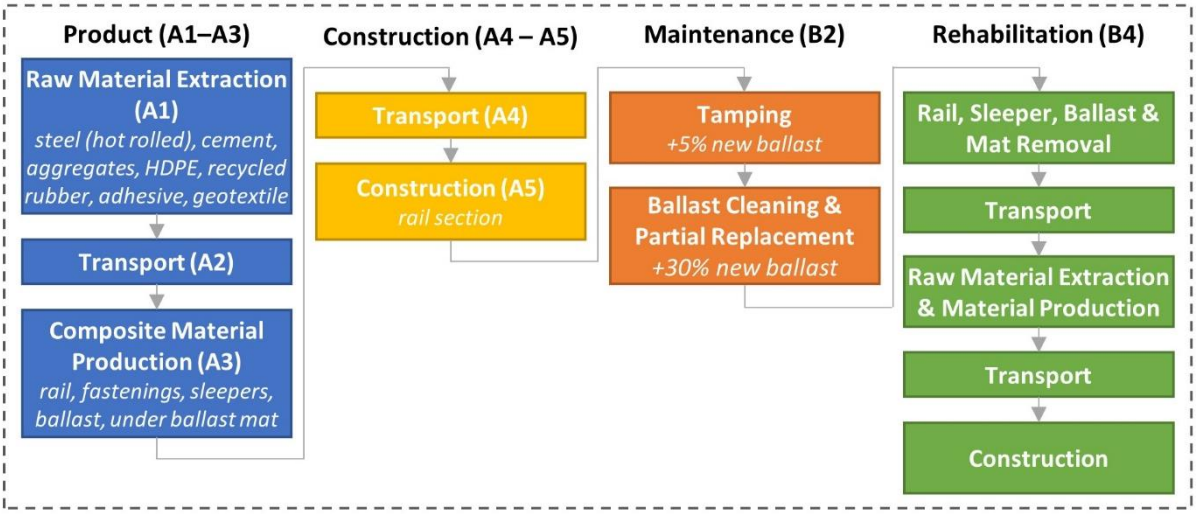

Figure 3. Boundary conditions for LCA and LCCA undertaken.

For this analysis, a functional unit (FU) of 1 km of 2-lane high-speed railway was considered. The railway design was based upon a local track section design between Granada-Toscón, supposing a traffic load of 20 Million Gross Tons (MGT). The railway track is composed of rails, rail pads, sleepers, fastening systems, and ballast. Per FU, this totalled to: 240 t of UIC-60 rail, 2.20 t of HDPE rail pads, 3333 AI-model sleepers, and 8736.50 t of granite ballast (0.34 m deep bed with an average width of 4.46 m, considering shoulders, plus 0.21 m thick layer added to surround the sleepers). The UBM and GridMats were selected to have a thickness of 7 mm according to the results from the previous sections. The subballast was considered to be beyond the scope of this study. The environmental impacts for the materials were taken from environmental product declarations. These are displayed in Appendix A, and were selected according to their quality and representativeness of the local region. EPDs were selected as the data sources given their suitability for construction LCAs [34]. Cost data was selected according to local prices, and they are also referenced in Appendix A.

The construction schedule was the same for the case study as the high-speed project selected. The steps simulated were: (1) transport of ballast to stockyard (40 km, with 400 hp 32 t truck), where half was then transported to site (10 km), spread, and compacted; (2) transport of sleepers to site (123 km, with 150 hp 12 t truck), where they were then laid; (3) spreading of remaining ballast (10 km, by train) and spread; (4) transport of rails to site (780 km, by train), followed by rail laying and fixing; (5) final tamping to prepare rail line, where four tamping operations were undertaken. Reference values for the productivity and working hours of the required machinery considered for the laying operations and compaction of all the elements involved were collected from [35].

The maintenance and rehabilitation frequencies were calculated from the results of the previous section. They were calculated according to the permissible settlements outlined in the previous section. The maintenance operations considered were ballast tamping, cleaning, and partial replacement. The productivity and fuel consumption data were collected from [34]. During the tamping operations, 5% new ballast was added to the track. The replacement operations considered the entire removal and replacement of the track, per FU. For all analyses, the "remaining service-life" (RSL) was considered, as recommended in other construction product category rules [36].

3. Analysis of Results and Discussion

The analysis of results carried out in this section focused on assessing the impact of aperture size for the orifices of the GridMat; the influence of density of apertures (number of voids per GridMat surface); frequency of maintenance and renewal operations in a period of 50 years; and results of the LCa and LCCA comparing the GridMat with the cases of sections with and without standard mats.

3.1. Impact of Aperture Size

Figure 4 shows the cumulative settlement and vertical stiffness modulus results obtained in the ballast box tests, reproducing full-scale track sections for the conventional reference (NM, marked with flat lines), standard under ballast mats (represented in the value of 0 mm of aperture size), and GridMat cases, with varying aperture sizes, assessing the influence of this design parameter. Figure 4a represents the case of the hard mats (7 mm thick), whereas Figure 4b presents the case of medium mats (11 mm thick).

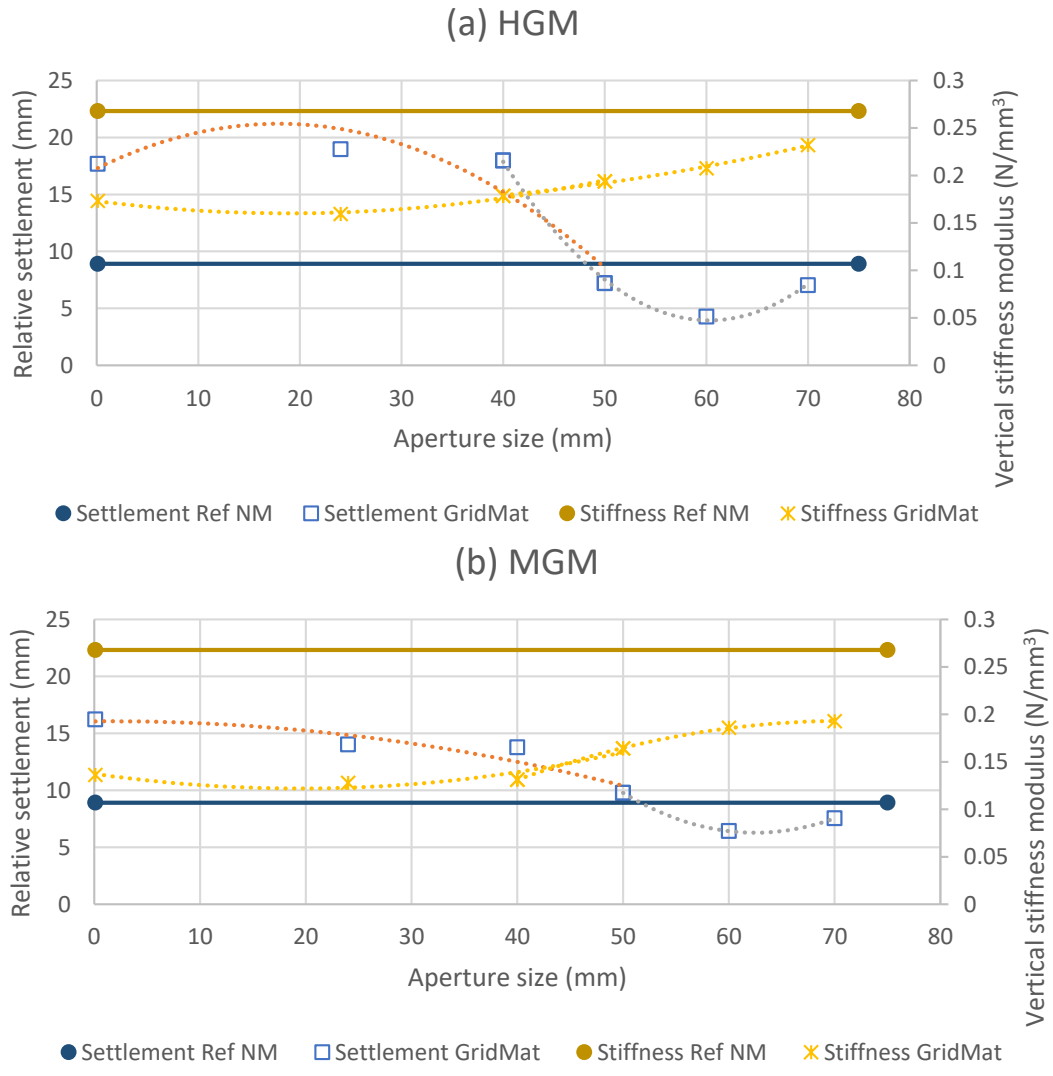

Figure 4. Settlement and stiffness results for hard (**a**) and medium (**b**) GridMats.

For both types of mats (hard and medium) it is seen that the aperture size has little influence up to values around 40 mm, confirming that mats with no voids (or little ones) led to higher ballast settlement than the reference case (with no mat—NM), as seen in previous studies [6,10,11]. Moreover, the results denote that the mats with apertures lower than 40 mm provided lower vertical stiffness modulus, allowing for increasing damping capacity.

On the other hand, results show that values higher than 40 mm for the diameter of the circular orifices led to a considerable reduction in ballast settlement. This could be associated with higher ability to confine ballast aggregates, as seen in previous studies [14]. In particular, it is seen that the settlement values reduced when increasing aperture size up to around 60 mm in diameter, but beyond this size led to a slight increase in settlement. In this sense, it can be seen that aperture values close to 60 mm resulted in settlement values lower than standard mats (less than 50%). This leads to even lower values than those from a conventional section without a mat, for both types of GridMat (HGM and MGM).

In addition, it was seen that the capacity to reduce section stiffness up to 40% when using standard mats (0 mm aperture size) was maintained with GridMat presenting aperture sizes lower than 50–60 mm. Meanwhile, higher sizes led to a slight reduction in section flexibility when compared with standard mats. Therefore, from these results, it could be said that an aperture size around 50–60 mm could be most appropriate for reducing track deformation while maintaining the flexibility capacity of the mats. This is in consonance with previous studies [14] stating that the optimal aperture size for geogrids could be around 55 mm.

For a deeper analysis of the influence of aperture size on track settlement in the long term, Figure 5 displays the results of SRLC (trend to settlement in mm/cycle) for the HGM (Figure 5a) and MGM (Figure 5b) in comparison with the reference case without a mat (NM) and the cases with standard UBM (0 mm aperture size). The results confirm that the values of aperture size lower than 40 mm present limited effect in comparison with standard mats (represented for the case of 0 mm aperture size), whereas higher values led to a considerable reduction in trend to settlement. Nonetheless, it must be noted that aperture sizes higher than 60 mm showed a slight increase in trend to settlement, which could be associated with excessive orifice size in comparison with aggregates size, and therefore, reducing confining effect. In detail, it is seen that the aperture size around 55 mm (established as a maximum in order to avoid a significant reduction in track flexibility) led to a settlement reduction of around 75%, in comparison with standard mats. The GridMats also obtained similar settlement values to those recorded for the reference case without a mat.

Therefore, based on Figures 4 and 5, these results confirm that the GridMat solution with 55 mm of aperture diameter could provide flexibility and damping capacity to a track section without leading to the phenomena of ballast destabilisation that could occur with standard mats. The settlement results are also comparable to those from the conventional section (with no UBM), but offer a solution without excessive stiffness, which could be more ideal for track sections such as bridges, tunnels, transitions areas, etc.

3.2. Influence of Density of Apertures (Void Area)

Considering the previous results for aperture size, Figure 6 displays the influence of void area with 55 mm apertures. The void area was varied depending on the distance between apertures per m^2. In this section, the hard mat was selected to study the influence of the void area. Figure 6a represents the impact on relative settlement during the tests and on the section stiffness, whereas Figure 6b displays the settlement results.

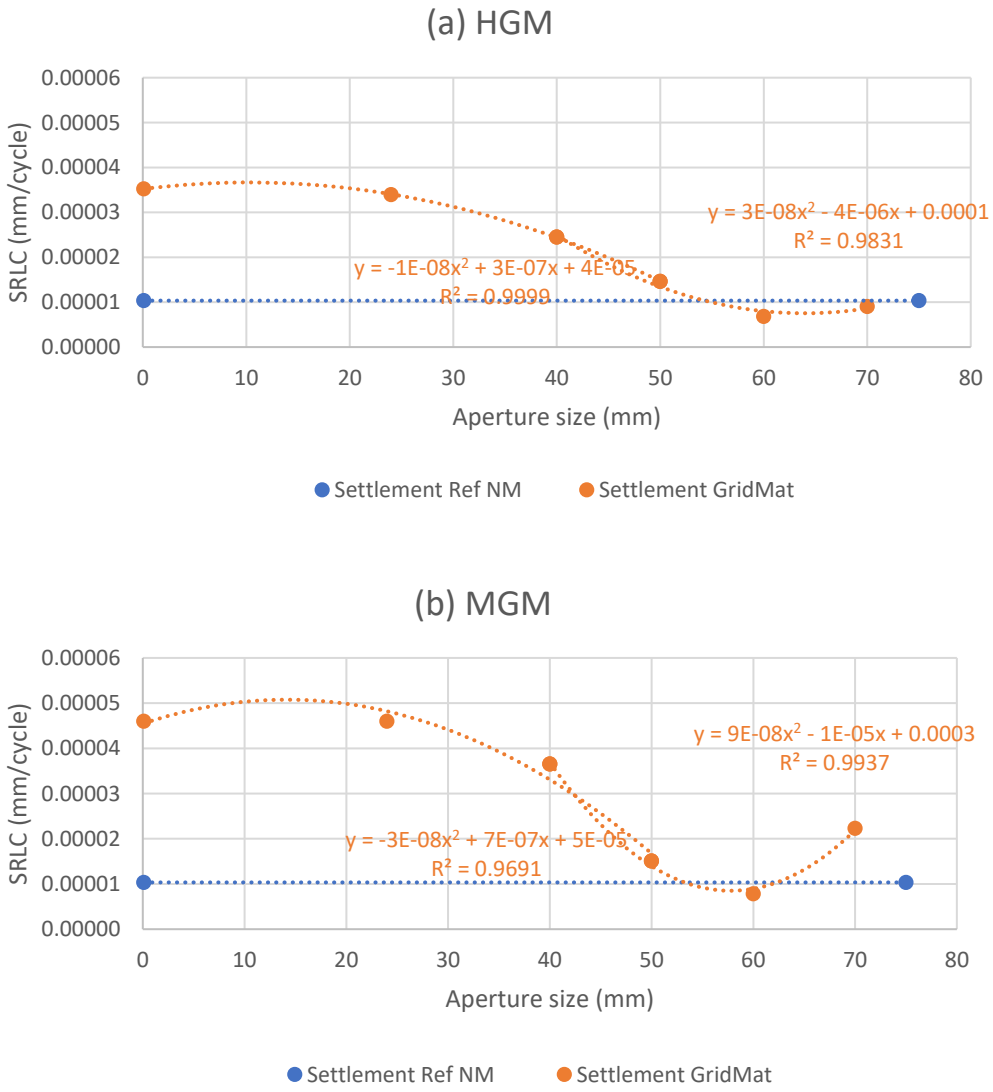

Figure 5. Settlement results for (**a**) hard and (**b**) medium GridMats according to aperture size.

The results reflect that an increase in number of apertures reduced the settlement and deformation up to values of around 25% of void area (corresponding to approximately 100 apertures per m^2). Beyond such a void area (25% of voids over total mat surface), little influence was seen in comparison with a reference section with no mat. On the other hand, the number of apertures led to a progressive increase in section stiffness due to the reduction in mat surface (the higher the number of apertures—Void area—the lower the surface of mat under the ballast layer), being accentuated from 25% of void area. Therefore, this parameter is seen to also play a key role in the design of GridMat, as it reduced the settlement while maintaining damping capacity. Therefore, it could be said that a 25% void area with 50 mm apertures could be appropriate for the objective of this study.

3.3. Prediction of Demand for Maintenance and Renewal Operations

With the aim of determining the impact of the GridMat on track quality and durability, Figure 7 shows the maintenance requirement results. Specifically, tamping (to correct longitudinal geometry), calculated from the box test results for the conventional track without a mat (NM), the hard under ballast mat (HM), and the GridMat (HGM) with 55 mm apertures around 2 cm apart (close to 100 voids per m^2). The results are expressed as maintenance frequency required per year depending on SD limits (maximum and minimum, from Table 2) at different speed ranges. Similarly, Figure 8 shows the predicted number of renewal operations required for each solution over 50 years (the selected analysis period).

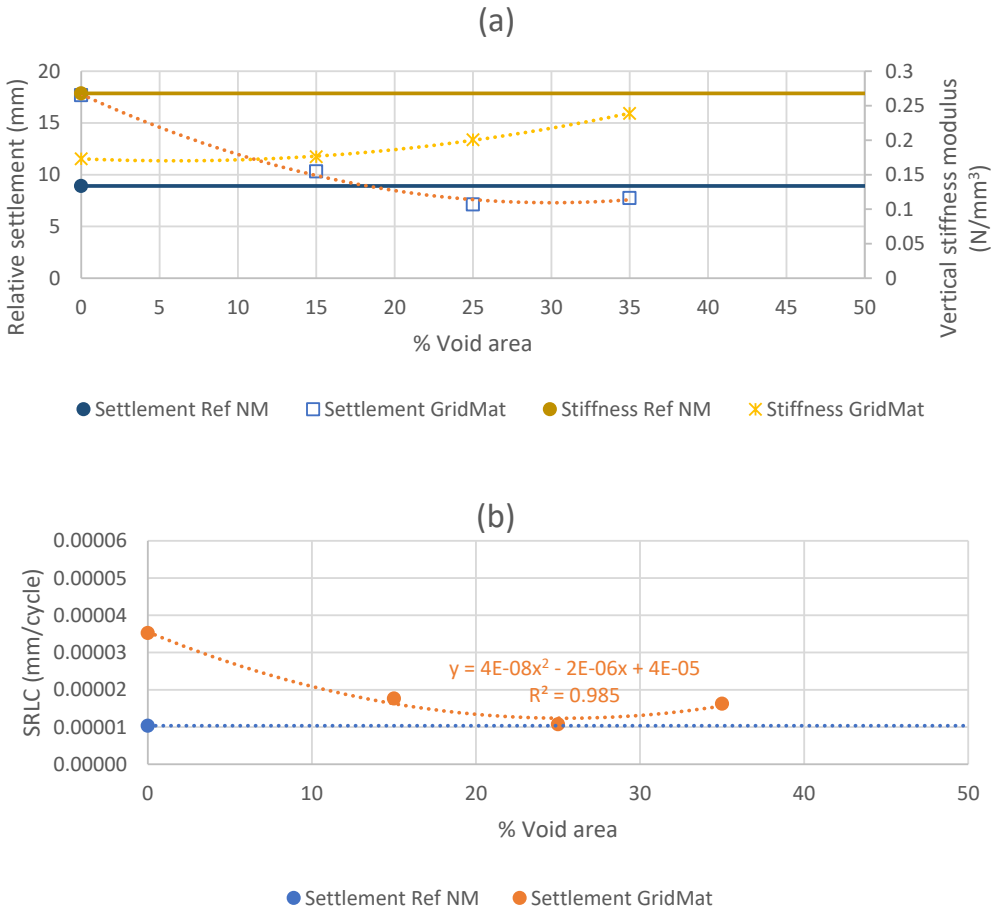

Figure 6. Influence of the density of orifices (void area) in GridMat. Results of (**a**) relative settlement at the end of the test and impact on section stiffness; and (**b**) influence on trend to settlement depending on void area.

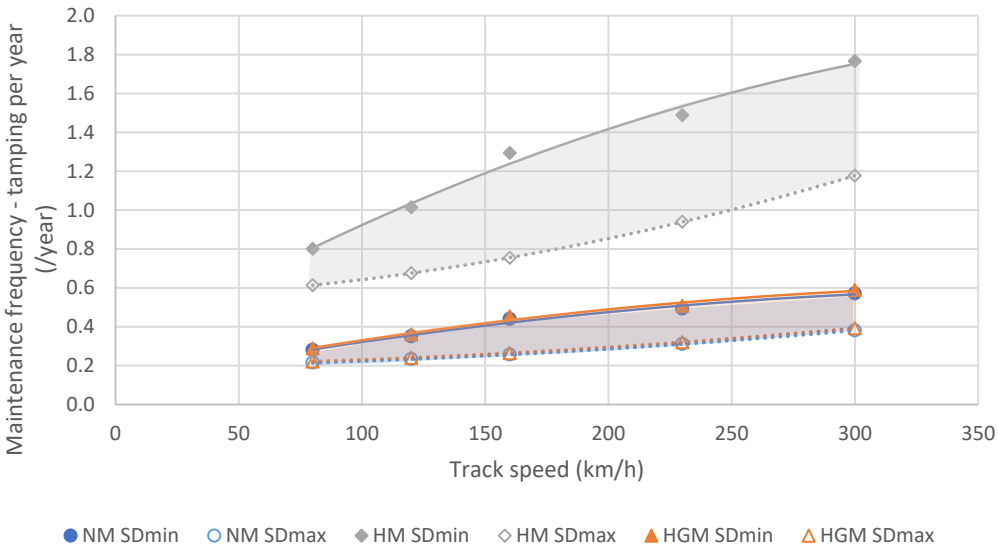

Figure 7. Maintenance frequency for a conventional track without a mat, with a UBM and with GridMats.

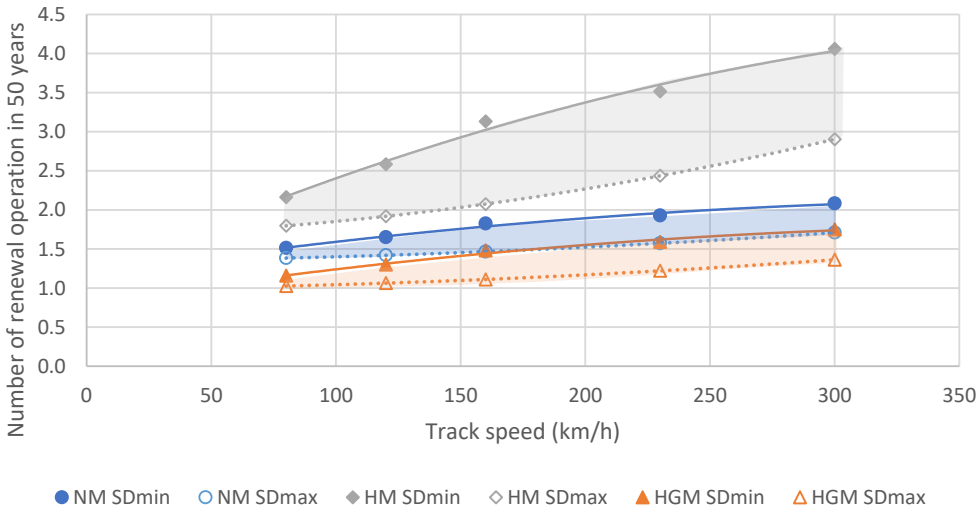

Figure 8. Maintenance requirements for considered tracks over a 50-year analysis period.

The results reflect that the application of the GridMat technology could considerably reduce the number of maintenance operations required (reductions of up to four times), in comparison with the standard HM case due to the decrease in track settlement when using the GridMat to avoid ballast destabilisation. In comparison to the case with no mat (NM) in conventional track sections, results state that this solution presents a similar need for geometrical corrections, while providing higher elasticity and flexibility as seen in previous results. Therefore, this means that the GridMat could satisfy the objective of using elastic solutions under ballast (provide damping capacity) without deriving in a possible increase in maintenance frequency if ballast destabilization takes places as a consequence of increasing particle oscillation.

Moreover, Figure 7 shows that the GridMat could allow for a considerable reduction (up to 25%) in need for renewal operations in the long-term, in comparison with conventional tracks without mats. This could be associated with the fact that this solution reduces the stress on the ballast layer, allowing for reduction in the degradation of particles under traffic, while reducing the need for maintenance and geometrical corrections. This also decreases particle degradation due to tamping operations.

3.4. Environmental and Economic Impacts

Figure 9 shows the initial construction and life-cycle maintenance and rehabilitation environmental and economic results for the 50-year analysis undertaken, for the conventional track, the under-ballast mat, and the GridMat cases studied. All cases are presented for a rail track which would function at 80 km/h and 300 km/h, as seen in the previous section. The results are broken down per life-cycle stage considered (A1–A3 product stage, A4–A5 construction, B2 maintenance and B4 renewal, according to the EN 15804 [33]).

From the initial construction results, it was found that the addition of both a conventional UBM and a GridMat would offer close to negligible detrimental impacts. Specifically, an increase of 0.33% in energy, 0.12% in GWP, and 1.88% in costs, compared to the reference rail track. Meanwhile, due to using less material, the GridMat would only require an increase in 0.25% in energy, 0.09% in GWP, and 1.41% in costs. This may be associated with the fact that the product stage (A1–A3) requires the largest amount of resources and funds, and so the addition of the mat was found to be minimal considering the rest of the material inventory required.

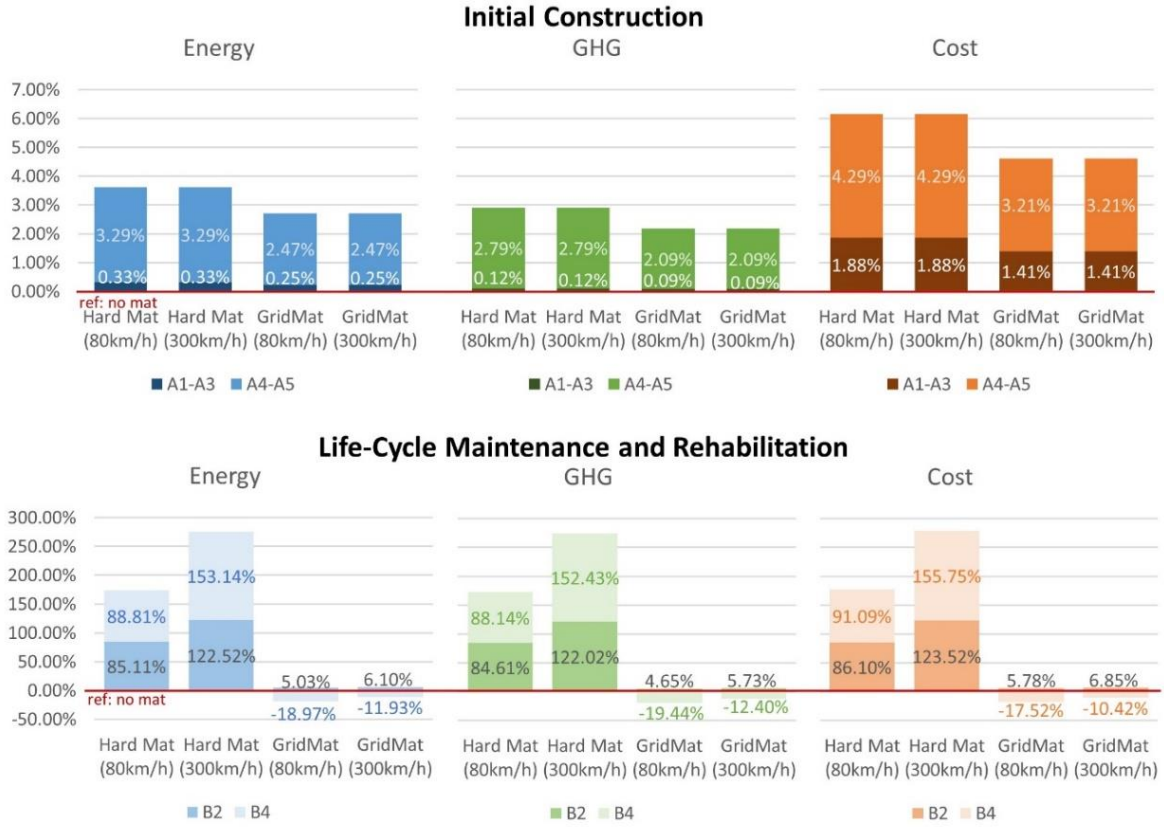

Figure 9. LCA and LCCA results for mat case studies, compared to conventional track.

Regarding the life-cycle, it is evident that the conventional under-ballast mat does cause ballast destabilisation and thus would require more maintenance operations to adhere to settlement requirements according to design standards. The conventional UBM would increase environmental impacts and cost requirements by 100.52% for the maintenance phase and between 16.97–17.16% and 18.61%, respectively, for the rehabilitation phase. Meanwhile, regarding the effect of the GridMat, it can be seen that for track maintenance (B2, i.e., tamping) the GridMat would not offer any specific reductions compared to the conventional track (3.10% in impacts and costs on average), given the ballast confinement. However, the GridMat design would offer noticeable environmental and economic reductions for track rehabilitation (B4—−21.01% in energy, −21.11% in GWP, and −20.28% in costs), as it would also reduce ballast degradation. Thus, considering the benefits of the GridMat over the life-cycle of the project, the use of the GridMat could be deemed favourable in the study undertaken.

4. Conclusions

The aim of this study was to develop a novel GridMat technology, which combined standard under-ballast mats with geo-grid designs, and tested their viability along the life-cycle of a rail track project. Through laboratory box tests and LCA and LCCA, the following conclusions were determined:

- Box tests demonstrated that GridMat with an aperture size of around 50–60 mm could be the most appropriate for reducing track deformation while providing damping capacity.
- Compared to standard mats (with no voids), GridMat could reduce up to 50% the settlement of railway ballasted track while maintaining the flexibility capacity of the mats (reducing around 40% the section stiffness when compared with reference track with no mats).
- It was proven that the number of voids per square meter of GridMat plays an essential role on performance and benefits.

- Void area up to around 25% of the mat (corresponding to approximately 100 voids per m^2 with aperture size of 55 mm) showed to be the optimal design to allow for reducing the trend to track settlement and deformation while providing damping and flexibility capacity.
- It was estimated that GridMat technology could reduce up to four times the tamping internals in comparison with standard mats while providing similar values to those from a conventional track with no mat causing ballast destabilisation. In addition, GridMat was found to provide a considerable reduction in the need for renewal operations over the life-cycle of the track.
- LCA and LCCA showed that GridMat allowed for reducing energy consumption, emissions, and costs when compared with standard mats (with no voids), particularly in the maintenance and rehabilitation periods where reductions of up to around 150% were found.
- Additionally, compared with tracks without elastic solutions under ballast, the GridMat design was found to offer a minimal increase (lower 5%) in environmental impacts and economic investment during the initial construction step while potentially offering around 20% savings over its whole life-cycle.

Through this study into design optimisation of the GridMat technology, it was possible to ascertain its environmental and economic benefits. It was found that the GridMat was most mechanically viable with 55 mm wide apertures occupying 25% of the total surface of UBM (corresponding to around 100 orifices per m^2). While providing a reduction in tamping requirements compared to the use of standard mats, significant savings were found across the life-cycle of the track. Nonetheless, further research will be carried out for optimizing the installation on GridMat while defining the most appropriate position into the ballast layer by considering installation, performance, and impact on operations for track maintenance.

Author Contributions: Conceptualization, M.S.-S.; methodology, M.S.-S. and J.M.C.-M.; software, T.M.; validation, F.M.-N. and M.C.R.-G.; formal analysis, M.S.-S.; investigation, J.M.C.-M. and T.M.; resources, M.C.R.-G.; data curation, T.M.; writing—original draft preparation, M.S.-S. and T.M.; writing—review and editing, M.S.-S.; visualization, F.M.-N.; supervision, M.C.R.-G.; project administration, M.S.-S.; funding acquisition, M.S.-S. and F.M.-N. All authors have read and agreed to the published version of the manuscript.

Funding: The present study has been conducted within the framework of the ECO-Smart Pads (Smart and Sustainable Resilient Pads for the Railway of the Future, RTI2018-102124-J-IOO) research project, funded by the Ministry of Economy and Competitiveness of Spain.

Conflicts of Interest: The authors declare no conflict of interest.

Appendix A. Life-Cycle Inventory

The environmental and cost data sources are provided in Table A1.

Table A1. Environmental and economic inventory sources.

Stage	Unit	Material/Process	Source	
			Energy/GWP	€
A1 & A3—raw material extraction & material production	t	Rail (hot-rolled steel)	Global EPD (2020) [37]	GIF (2003) [38]
	t	Rail pad (HDPE)	PlasticsEurope (2014) [39]	Local provider
	unit	Sleeper (pre-cast concrete)	International EPD System (2017) [40]	GIF (2003) [38]

Table A1. *Cont.*

Stage	Unit	Material/Process	Source	
			Energy/GWP	**€**
	t	Ballast (crushed granite)	BRE Global (2018a; 2018b) [41,42]	GIF (2003) [38]
	m^2	Under-ballast mat	International EPD System (2021) [43]	Local provider
A2 & A4—Transportation	t-km	Truck transportation	Ecoinvent: transport, freight, lorry >32 metric ton, EURO6, GLO	Project data
			Ecoinvent: transport, freight, lorry 16–32 metric ton, EURO6, GLO	Project data
		Train	Ecoinvent: transport, freight train, electricity, GLO	Project data
A5—Construction	km	Loader	Ecoinvent: machine operation, diesel, ≥74.57 kW, low load factor, GLO	Project data
		Ballast spreader	Kiani et al. (2008) [35]	Project data
		Sleeper laying machine	Kiani et al. (2008) [35]	Project data
B2	km	Tamping machine	Kiani et al. (2008) [35]	Project data
		Ballast changing machine	Kiani et al. (2008) [35]	Project data
		Ballast cleaning machine	Kiani et al. (2008) [35]	Project data
B4	-	*Same as A1–A5*		

References

1. Union International of Railway. *Recommendations for the Use of under Ballast Mats*; UIC Code 719-1; Union International of Railway: Paris, France, 2011.
2. Sol-Sánchez, M.; Moreno-Navarro, F.; Rubio-Gámez, M.C. The use of elastic elements in railway tracks: A state of the art review. *Constr. Build. Mater.* **2015**, *75*, 293–305. [CrossRef]
3. Xin, T.; Ding, Y.; Wang, P.; Gao, L. Application of rubber mats in transition zone between two different slab tracks in high-speed railway. *Constr. Build. Mater.* **2020**, *243*, 118219. [CrossRef]
4. Zheng, W.; Sheng, X.; He, H.; Xu, H.; Yang, Y. Use of Rubber Mat to Improve Deformation Behaviors of Ballastless Tracks Laid on Bridges. *Adv. Civ. Eng.* **2020**, *2020*, 8821402. [CrossRef]
5. Lapcik, L.; Augustin, P.; Pištěk, A.; Bujnoch, L. Measurement of the dynamic stiffness of recycled rubber based railway track mats according to the DB-TL 918.071 standard. *Appl. Acoust.* **2001**, *62*, 1123–1128. [CrossRef]
6. Sol-Sánchez, M.; Moreno-Navarro, F.; Rubio-Gámez, M.C. The Use of Deconstructed Tires as Elastic Elements in Railway Tracks. *Materials* **2014**, *7*, 5903–5919. [CrossRef] [PubMed]
7. Horníček, L.; Lidmila, M. Simulation of long-term behaviour of antivibration mats from rubber recyclate by means of cyclic loading. In Proceedings of the International Conference on Modelling and Simulation, Prague, Czech Republic, 22–25 June 2010.
8. Kraśkiewicz, C.; Zbiciak, A.; Al Sabouni-Zawadzka, A.; Marczak, M. Analysis of the influence of fatigue strength of prototype under ballast mats (UBMs) on the effectiveness protection against vibration caused by railway traffic. *Materials* **2021**, *14*, 2125. [CrossRef] [PubMed]
9. Raymond, G.P.; Bathurst, R.J. Performance of large-scale model single tie-ballast systems. *Transp. Res. Rec.* **1987**, *1134*, 7–14.
10. Sol-Sánchez, M.; Moreno-Navarro, F.; Rubio-Gámez, M.C.; Manzo, N.; Fontserè, V. Full-scale study of Neoballast section for its application in railway tracks: Optimization of track design. *Mater. Struct.* **2018**, *51*, 43. [CrossRef]
11. Kumar, N.; Suhr, B.; Marschnlg, S.; Dietmaler, P.; Marte, C.; Six, K. Micro-mechanical investigation of railway ballast behavior under cyclic loading in a box test using DEM: Effects of elastic layers and ballast types. *Granul. Matter.* **2019**, *21*, 106. [CrossRef]
12. Hussaini, S.K.K.; Indraratna, B.; Vinod, J.S. Performance assessment of geogrid-reinforced railroad ballast during cyclic loading. *Transp. Geotech.* **2015**, *2*, 99–107. [CrossRef]
13. Esmaeili, M.; Zakeri, J.A.; Babaei, M. Laboratory and field investigation of the effect of geogrid-reinforced ballast on railway track lateral resistance. *Geotext. Geomembr.* **2017**, *45*, 23–33. [CrossRef]

14. Brown, S.F.; Kwan, J.; Thom, N.H. Identifying the key parameters that influence geogrid reinforcement of railway ballast. *Geotext. Geomembr.* **2007**, *25*, 326–355. [CrossRef]
15. Indraratna, B.; Hussaini, S.K.K.; Karimullah, S.K.; Vinod, J.S. On the shear behavior of ballast-geosynthetic interfaces. *Geotech. Test. J.* **2012**, *35*, 305–312.
16. Indraratna, B.; Hussaini, S.K.K.; Vinod, J.S. The lateral displacement response of geogrid-reinforced ballast under cyclic loading. *Geotext. Geomembr.* **2013**, *39*, 20–29. [CrossRef]
17. *DIN 45673-5:2010-08*; Mechanical Vibration. Resilient Elements Used in Railway Tracks. Part 5: Laboratory Test Procedures for Under-Ballast Mats. DIN: Berlin, Germany, 2010.
18. *DBS 918 071-01*; Unterschottermatten zur Minderung der Schotterbeanspruchung. Deutsche Bahn: Munich, Germany, 2010.
19. Taheri, V.; Fakhri, M.; Hayati, P. Evaluation of airfield concrete block pavements based on 3-D modelling and plate loading test. *Constr. Build. Mater.* **2021**, *280*, 122441. [CrossRef]
20. *EN 13146-9:2011*; Railway Applications. Track. Test Methods for Fastening Systems. Part 9: Determination of Stiffness. European Committee for Standardization: Brussels, Belgium, 2009.
21. *EN 13450*; Aggregates for Railway Ballast. European Committee for Standardization. Asociación Española de Normalización y Certificación: Madrid, Spain, 2003.
22. Sol-Sánchez, M.; Pirozzolo, L.; Moreno-Navarro, F.; Rubio-Gámez, M.C. A study into the mechanical performance of different configurations for the railway track section: A laboratory approach. *Eng. Struct.* **2016**, *119*, 13–23. [CrossRef]
23. Sol-Sánchez, M.; Moreno-Navarro, F.; Rubio-Gámez, M.C. An alternative sustainable railway maintenance technique based on the use of rubber particles. *J. Clean. Prod.* **2017**, *142*, 3850–3858. [CrossRef]
24. Wilk, S.; Stark, T.; Rose, J. Evaluating tie support at railway bridge transitions. *Proc. Inst. Mech. Eng. F J. Rail Rapid.* **2016**, *230*, 1336–1350. [CrossRef]
25. Sussman, T. Field conditions observed at a site with concrete tie base abrasion. In Proceedings of the Railway Engineering, Conference at Edinburg, Edinburgh, UK, 21–22 June 2017.
26. D'Angelo, G.; Bressi, S.; Giunta, M.; Lo Presti, D.; Thom, N. Novel performance-based technique for predicting maintenance strategy of bitumen stabilized ballast. *Constr. Build. Mater.* **2018**, *161*, 1–8. [CrossRef]
27. *EN 13848-5:2020*; Railway Applications—Track—Track Geometry Quality—Part 5: Geometric Quality Levels—Plain Line. Engineering Sustainability 161 Issue ES2 Environmental Life-Cycle Assessment of Railway Track. Asociación Española de Normalización y Certificación: Madrid, Spain, 2020.
28. Pires, J. *Integrated Maintenance Model for Heavy Haul Tracks*; Ecole Polytechnique Federale de Lausanne: Lausanne, Switzerland, 2016.
29. Audley, M.; Andrews, J. The effects of tamping on railway track geometry degradation. *Proc. Inst. Mech. Eng. Part F J. Rail Rapid. Transit.* **2013**, *227*, 376–391. [CrossRef]
30. Selig, E.T.; Waters, J.M. *Track Geotechnology and Substructure Management*; Telford, T., Ed.; Thomas Telford Ltd.: London, UK, 1994.
31. Sol-Sánchez, M.; Moreno-Navarro, F.; Rubio-Gámez, M.C. Analysis of ballast tamping and stoneblowing processes on railway track behaviour: The influence of using USPs. *Géotechnique* **2015**, *66*, 481–489. [CrossRef]
32. Nurmikolu, A. *Degradation and Frost Susceptibility of Crushed Rock Aggregates Used in Structural Layers of Railway Track*; Tampere University of Technology: Tampere, Finland, 2005.
33. *EN 15804:2012+A1:2020*; Sustainability of Construction Works—Environmental Product Declarations—Core Rules for the Product Category of Construction Products. Asociación Española de Normalización y Certificación: Madrid, Spain, 2020.
34. Rangelov, M.; Dylla, H.; Mukherjee, A.; Sivaneswaran, N. Use of environmental product declarations (EPDs) of pavement materials in the United States of America (USA) to ensure environmental impact reductions. *Clean. Prod.* **2020**, *283*, 124619. [CrossRef]
35. Kiani, M.J.; Parry, T.; Ceney, H. Environmental life-cycle assessment of railway track beds. *Proc. Inst. Civ. Eng. Eng. Sustain.* **2008**, *161*, 135–142. [CrossRef]
36. Federal Highway Administration. *Life-Cycle Cost Analysis Primer*; U.S. Department of Transportation Federal Highway Administration Office of Asset Management: Washington, DC, USA, 2002.
37. Global EPD. Productos Largos de Acero no Aleado para Construcción Laminados en Caliente Procedentes de Horno Eléctrico: Perfiles Estructurales de uso General, Barras y Perfiles Comerciales. AENOR. Código GlobalEPD: 001-003 Renovación 1. 2020. Available online: https://www.aenor.com/Producto_DAP_pdf/GlobalEPD_001_003_r2_ESP.pdf (accessed on 24 July 2022).
38. GIF. *Base de Precios Tipo para los Proyectos de Vía. Gestor de Infraestructuras Ferroviarias*; GIF: Madrid, Spain, 2003.
39. PlasticsEurope. Eco-Profiles and Environmental Product Declarations of the European Plastics Manufacturers. High-Density Polyethylene (HDPE), Low-Density Polyethylene (LDPE), Linear Low-Density Polyethylene (LLDPE). 2014. Available online: https://www.pedagogie.ac-aix-marseille.fr/upload/docs/application/pdf/2015-11/4-_eco-profile_pe_2014-04.pdf (accessed on 24 July 2022).
40. International EPD System. Environmental Product Declaration for Railway Sleepers SB35F and SBR25ML. S-P-01060. 2017. Available online: https://api.environdec.com/api/v1/EPDLibrary/Files/f163cd3c-595d-4338-b95d-2cf13c9e0177/Data (accessed on 24 July 2022).
41. BRE Global. Environmental Product Declaration for Granite Aggregate—Glensanda. BREG EN EPD No.: 000205. 2018a. Available online: https://www.aggregate.com/sites/aiuk/files/atoms/files/glensanda_epd.pdf (accessed on 24 July 2022).

42. BRE Global. Environmental Product Declaration for Granite Aggregate—Bardon Hill. BREG EN EPD No.: 000206. 2018b. Available online: https://www.aggregate.com/sites/aiuk/files/atoms/files/bardon_hill_epd.pdf (accessed on 24 July 2022).
43. International EPD System. Environmental Product Declaration for Under Ballast Mat, Type UBM-H35-C. S-P-02061. 2021. Available online: https://api.environdec.com/api/v1/EPDLibrary/Files/00d2ff8a-5520-48ce-054f-08d9b9685fa2/Data (accessed on 24 July 2022).